Submitted: 28 April, 2023 Accepted: 12 June, 2023 Published: 08 July, 2023 DOI:10.22514/sv.2023.065

Open Access
Signa Vitae

ORIGINAL RESEARCH

HOMER1A restores sevoflurane-induced cognitive dysfunction by regulating microglia's activation through activating the AMPK/TXNIP axis

Guangzhen Zhao[1], Jianmin Jing[2,*]

[1]Department of Neurology, Beijing Longfu Hospital, 100010 Beijing, China
[2]Department of Anesthesia, ShanXi Provincial People's Hospital, 030012 Taiyuan, Shanxi, China

***Correspondence**
jingjianmin_dr66@163.com
(Jianmin Jing)

Abstract

More and more researchers have discovered that the employment of anesthetics can lead to cognitive dysfunction of brain. *HOMER1A* has been investigated to have neuroprotective effects. Sevoflurane (SEV) is the most common inhaled anesthetic utilized in surgery, but the role of *HOMER1A* in SEV-induced cognitive dysfunction is unclear. Thus, in this study, SEV was utilized in our study for investigating the role of *HOMER1A*. At first, the rat model was established through inhaling 2% SEV. Results from our study uncovered that the brain tissues of SEV-treated rats were severely damaged, and the levels of S-100β and neuron-specific enolase (NSE) were markedly elevated after SEV treatment. Further study showed that *HOMER1A* exhibited lower expression in the brain tissues of SEV-mediated rats. In addition, *HOMER1A* ameliorated nerve injury and cognitive deficit in SEV-treated rats. Moreover, *HOMER1A* improved inflammation in the brain tissues of SEV-induced rats. *HOMER1A* suppressed SEV-stimulated microglial activation through modulating M1/M2 polarization. Besides, *HOMER1A* activated Adenosine 5'-monophosphate (AMP)-activated protein kinase (AMPK) pathway to reduce thioredoxin interacting protein (TXNIP) expression. Finally, through rescue assays, inhibition of AMPK activation (Compound C (CC) treatment) attenuated the neuroprotective effects of *HOMER1A* in SEV-triggered rats. In summary, *HOMER1A* regulated microglia M1/M2 polarization to restore SEV-stimulated cognitive dysfunction through activating the AMPK/TXNIP axis.

Keywords

HOMER1A; Sevoflurane; Cognitive dysfunction; M1/M2 polarization; AMPK/TXNIP axis

1. Introduction

Postoperative cognitive dysfunction (POCD) is a fearful neurological complication, with the subtle declines in memory, attention, and information processing speed after surgery with anesthesia [1, 2]. This phenomenon generally occurs in older people [3]. SEV is the most common inhaled anesthetic applied in surgery [4]. At present, some investigations have discovered that sevoflurane (SEV) induced cytotoxicity may cause cognitive impairment in humans and animals [5].

More and more studies focus on the targeted proteins which modulate SEV-triggered cognitive dysfunction. For example, knockdown of cyclin dependent kinase 5 (*CDK5*) enhances sirtuin 1 (*SIRT1*)-stimulated autophagy to alleviate SEV-mediated cognitive dysfunction [6]. Dexmedetomidine regulates microRNA-129/toll-like receptor 4 (*TLR4*) axis to ameliorate SEV-mediated postoperative cognitive dysfunction [7]. In addition, lncRNA Rian targets miR-143-3p/LIM domain kinase 1 (*LIMK1*) axis to mitigate SEV anesthesia-stimulated cognitive dysfunction [8]. Methyltransferase like 3 (*METTL3*) affects N6-methyladenosine methylation to modulate hippocampal gene transcription in SEV-mediated postoperative cognitive dysfunction [9]. Therefore, searching effective target proteins for SEV-mediated cognitive dysfunction is the goal of many researchers.

HOMER1A is a member of the postsynaptic density protein family, which exhibits crucial roles in neuronal synaptic activity and is widely involved in neurological diseases [10, 11]. *HOMER1A* has been revealed to possess neuroprotective effects, and its upregulation can reduce cell apoptosis caused by traumatic neuronal injury and enhance protective autophagy, thereby alleviating brain injury [12]. In I/R-induced retinal ganglion cells, upregulation of *HOMER1A* mitigates cell apoptosis by reducing p-ERK levels, thus relieving I/R-stimulated visual impairment [13]. In addition, overexpression of *HOMER1A* has the effects of relieving depression [14]. Moreover, *HOMER1A* also suppresses inflammation, and in

the spine of mice, knockdown of *HOMER1A* facilitates inflammatory processes and exacerbates inflammatory pain [15]. However, the role of *HOMER1A* in modulating anesthetic-induced cognitive impairment remains unclear.

Under pathological conditions, activated microglia are existed, and named microglia polarization. Microglial activation is separated into two major phenotypes: classical activation (M1 phenotype) and substitution activation (M2 phenotype) [16]. M1 microglia releases some factors to suppress tissue repair, break the blood-brain barrier, and result into neuronal degeneration [17]. Conversely, M2 microglia owns anti-inflammatory effects and strengthen tissue repair [17]. Therefore, reducing M1 microglia and enhancing M2 microglia in POCD have great value. However, the regulatory effects of *HOMER1A* on M1/M2 polarization in POCD keep unclear.

This study aims to probe the effects of *HOMER1A* on SEV-stimulated cognitive dysfunction. Our results indicated that *HOMER1A* regulated AMPK/TXNIP axis activity, maintained the balance of glial M1/M2 phenotype and reduced neuroinflammation to restore SEV-induced cognitive impairment. These findings may contribute for the treatment of SEV-stimulated cognitive dysfunction.

2. Materials and methods

2.1 Animal study

The male Sprague-Dawley rats (n = 42, 260–280 g, 15 months) were acquired from Vital River Laboratory Animal Technology Co. Ltd. (Beijing, China). All rats were kept in individual cages, and given free water and food under a 12-h light/dark cycle for one week for environmental adaptation. This study was approved by the Animal Care and Use Committee of Shanxi Provincial People's Hospital.

To construct adeno-associated virus (AAV) vector, *HOMER1A* cDNA sequence was cloned into the multi cloning site (MCS) of pAAV-CAGGS-EGFP-P2A-MCS plasmid [18]. In general, the AAV vectors pHelper (Cell BioLabs, San Diego, CA, USA) and pAAV-DJ (Cell BioLabs) were transfected into the HEK293 cells. Post incubation for 3 days, the cells were collected, and the AAV titers were estimated through real time-quantitative polymerase chain reaction (RT-qPCR). Rats were anesthetized with tribromoethanol (250 mg/kg) and placed in a stereotactic frame (David Kopf, Tujunga, CA, USA). The AAV virus (0.5 μL, 1.0 $\times$ 10^{11} genome copies/mL) was injected into the hippocampus through a glass microinjection capillary tube at a rate of 0.1 μL/min (0.5 μL/site, six sites). The rates relative to the bregma were as followed (in mm): −2.0, ±1.8, −2.2; −2.0, ±1.8, −1.7; −2.8, ±3.0, −3.0.

HOMER1A: (sequence: GGAATCAGCAGGAGGAGATCT) [12].

The rats were randomly separated into 7 groups:

(1) rats (n = 6) were set in the blank control group (Sham group); (2) rats (n = 6) were anesthetized in 2% SEV for 5 h to set in the SEV group (SEV group); (3) rats (n = 6) were injected with AAV-NC in the Sham + AAV-NC group; (4) rats (n = 6) were injected with AAV-HOMER1A in the Sham + AAV-HOMER1A group; (5) rats (n = 6) induced by SEV were injected with AAV-NC in the SEV + AAV-NC group; (6) rats (n = 6) induced by SEV were injected with AAV-HOMER1A in the SEV + AAV-HOMER1A group; (7) rats (n = 6) induced by SEV were injected with AAV-HOMER1A and treated with CC (20 mg/kg, AMPK inhibitor) in the Sham + AAV-HOMER1A + CC group. The Morris water maze (MWM) test was utilized to evaluate their behaviors and functions of learning and memory. At last, rats were sacrificed by intraperitoneal anesthesia with pentobarbitone (800 mg/kg). Half of the rats' brain tissue was fastened in 4% paraformaldehyde, and the other half was kept in liquid nitrogen.

2.2 H&E staining

The brain tissues fastened in paraformaldehyde were dehydrated through different concentrations of alcohols, followed by paraffin-embedding. Next, tissues were cut into 4-μm thick sections, and then dyed with hematoxylin for 5 min and eosin for 30 s. The light microscope (BX53T-32P01, Olympus Corporation, Tokyo, Japan) was utilized to observe the pathological changes of the brain.

2.3 Morris water maze (MWM) test

The MWM test was utilized to evaluate the learning and memory abilities of rats. The acquisition test was done for 4 days (twice a day). On the 5th day, the spatial probe test was carried out. The learning and memory abilities in rats were evaluated through the acquisition test. At the fixed entry point of each quadrant, rats were put into the water in random order. The time of searching in the water and climbing on the platform was deemed as the escape latency, and rats kept on the platform for more than 3 s. If rats don't climb the platform within 120 seconds, manually guide them to the platform with a stick and made them to stay the platform for 30 s, and then put them back into the cage for the next test. The spatial memory ability of rats was evaluated through spatial probe method. After removing the platform from the pool, at the opposite side of the original target quadrant, the rats were put into the water and permitted to seek the platform. We recorded the number of passing through the platform within 120 s and counted the proportion (the time in the original target quadrant/the total time).

2.4 ELISA

Enzyme-linked immunosorbent assay (ELISA) was conducted to confirm the levels of brain injury markers (S-100β and NSE) and inflammatory factors (tumor necrosis factor-α (TNF-α), Interleukin-6 (IL-6) and Interleukin-1β (IL-1β)) in serum. The S-100β (SEA567Ra, USCN, USA), the neuron-specific enolase (NSE) (SEA537Ra, USCN), TNF-α (SEA133Si, USCN), IL-6 (SEA079Ra, USCN) and IL-1β (CSB-E08055r, CUSABIO) were measured through commercial ELISA kits in line with the manufacturer's instructions.

2.5 RT-qPCR

The extraction of RNAs was conducted using Trizol. Then, the reverse transcription of the RNAs to cDNAs was executed

using the reverse transcription kit (RR037A, Takara, Kyoto, Japan). Real-time quantitative PCR was carried out using the SYBR Premix PCR kit (RR820B, Takara, Kyoto, Japan). The $2^{-\triangle\triangle Ct}$ method was utilized for the calculation the relative expression of HOMER1A, TNF-α, IL-6, IL-1β, with normalizing to glyceraldehyde-3-phosphate dehydrogenase (*GAPDH*, the internal standard). The primers were presented as follows:

HOMER1A
F: 5′-ATAGCACCATCACTCCAAA-3′,
R: 5′-GAATCCCAGTCCATAAACA-3′;
TNF-α
F: 5′-AGCCGATGGGTTGTACCT-3′,
R: 5′-TGAGTTGGTCCCCCTTCT-3′;
IL-6
F: 5′-TCCAGTTGCCTTCTTGGGAC-3′,
R: 5′-GTACTCCAGAAGACCAGAGG-3′;
IL-1β
F: 5′-CCAGCTTCAAATCT CACAGCAG-3′,
R: 5′-CTTCTTTGGGTATTGCTTGGGATC-3′;
GAPDH
F: 5′-CAAGTTCAACGGCACAG-3′,
R: 5′-CCAGTAGACTCCACGACAT-3′.

2.6 Western blot

The proteins from brain tissues of rats extracted by RIPA lysis buffer (89900, Thermo Fisher Scientific, Inc., Waltham, MA, USA) were separated onto 10% sodium dodecyl sulfate-polyacrylamide gel electrophoresis (SDS-PAGE) and then transferred onto polyvinylidene fluoride (PVDF) membranes (Millipore, Billerica, MA). After blocked by skim milk, the membranes were incubated with primary antibodies at 4 °C for overnight. Next, the membranes were incubated with horseradish peroxidase (HRP)-conjugated secondary antibodies (ab7090, 1:2000, Abcam) for 1 h. Lastly, the chemiluminescence detection kit (89880, Thermo Fisher Scientific, Inc., Waltham, MA, USA) was utilized for the evaluation of the protein bands. The primary antibodies used in this study included: anti-HOMER1A (1:1000, ab184955, Abcam, Shanghai, China), anti-p-NF-κB p65 (1:1000, ab239882, Abcam), anti- nuclear factor kappa-B (NF-κB) p65 (0.5 μg/mL, ab16502, Abcam), anti-Iba1 (1 μg/mL, ab5076, Abcam), anti-CD16 (1:1000, ab211151, Abcam), anti-iNOS (1:1000, ab178945, Abcam), anti-CD206 (1 μg/mL, ab64693, Abcam), anti-Arg1 (1:1000, ab96183, Abcam), anti-p-AMPK (1:1000, ab131357, Abcam), anti-AMPK (1:1000, ab32047, Abcam), anti-TXNIP (1:1000, ab188865, Abcam), anti-P2RY12 (1:2000, ab184411, Abcam), anti-TMEM119 (1:1000, ab209064, Abcam) and anti-β-actin (1 μg/mL, ab8226, Abcam).

2.7 Immunofluorescence (IF) assay

The deparaffinized brain tissue sections were rehydrated. After washed with phosphate buffered saline (PBS), the antigen retrieval of sections was conducted through 0.1 M sodium citrate. Next, the sections were incubated with anti-Iba1, anti-GFAP, anti-MBP antibodies for overnight at 4 °C. After rinsed with PBS, the sections were incubated with fluorescence-labeled secondary antibodies. The nuclear was stained with 4,6-diamino-2-phenyl indole (DAPI), and the immunoreactivity was assessed through a fluorescence microscope (BX53T-32P01, Olympus, Tokyo, Japan).

2.8 TUNEL assay

The cell apoptosis was measured in brain tissues by using the *in situ* Cell Death Detection kit (11684817910, Roche, Basel, Switzerland). After staining, the images were randomly acquired in 5 fields under a fluorescence microscope (E200, Nikon, Tokyo, Japan). The cell apoptosis was evaluated by TUNEL-positive cells (%).

2.9 Flow cytometry

The Annexin V-FITC/PI Apoptosis Detection Kit (40302ES60, YEASEN, Shanghai, China) was used to examine the cell apoptosis according to the manufacturer's protocol. The brain tissue single-cell suspensions were incubated on ice for 0.5 h with the corresponding antibodies: CD16 (PE, 12-0161-82, eBioscience, USA), Iba1 antibody (Alexa Fluor® 568, ab221003, Abcam, UK) and arginase 1 (Alexa Fluor 700, 12-0161-82, eBioscience, USA). Next, Annexin V-FITC and PI were mixed with cell suspension for 15 min in dark. At last, cells were analyzed through flow cytometer (BD FACSAria II, BD, Franklin Lake, NJ, USA).

2.10 Statistical analysis

The data were displayed as mean $\pm$ standard deviation (SD). The SPSS 19.0 software (SPSS Inc., Chicago, IL, USA) was used for statistical analysis. Comparisons among groups (two or more) were done through the student's *t*-test or one-way analysis of variance (ANOVA) analysis. The $p < 0.05$ was set as statistically significant.

3. Results

3.1 *HOMER1A* exhibited lower expression in the brain tissues of SEV-mediated rats

The schematic of the timeline was showed in Fig. 1A. Rats were treated with SEV (2% for 5 h) at Day 0, and rats were killed at Day 5 to collect the blood and tissues for following experiments. As displayed in Fig. 1B, compared with the Sham group, the brain tissues of SEV-treated rats were severely damaged, and showed the increased number of dead cells with cytoplasm atrophy and nuclear degeneration. In addition, through TUNEL assay, cell apoptosis was enhanced by SEV treatment (Fig. 1C). Additionally, the levels of S-100β and NSE were markedly elevated after SEV treatment (Fig. 1D). The mRNA and protein expressions of HOMER1A were reduced in the SEV group (Fig. 1E,F). These data indicated that *HOMER1A* exhibited lower expression in the brain tissues of SEV-mediated rats.

3.2 *HOMER1A* ameliorated nerve injury and cognitive deficit in SEV-treated rats

The schematic of the timeline was showed in Fig. 2A. AAV-NC or AAV-HOMER1A was injected into the rats. Rats were

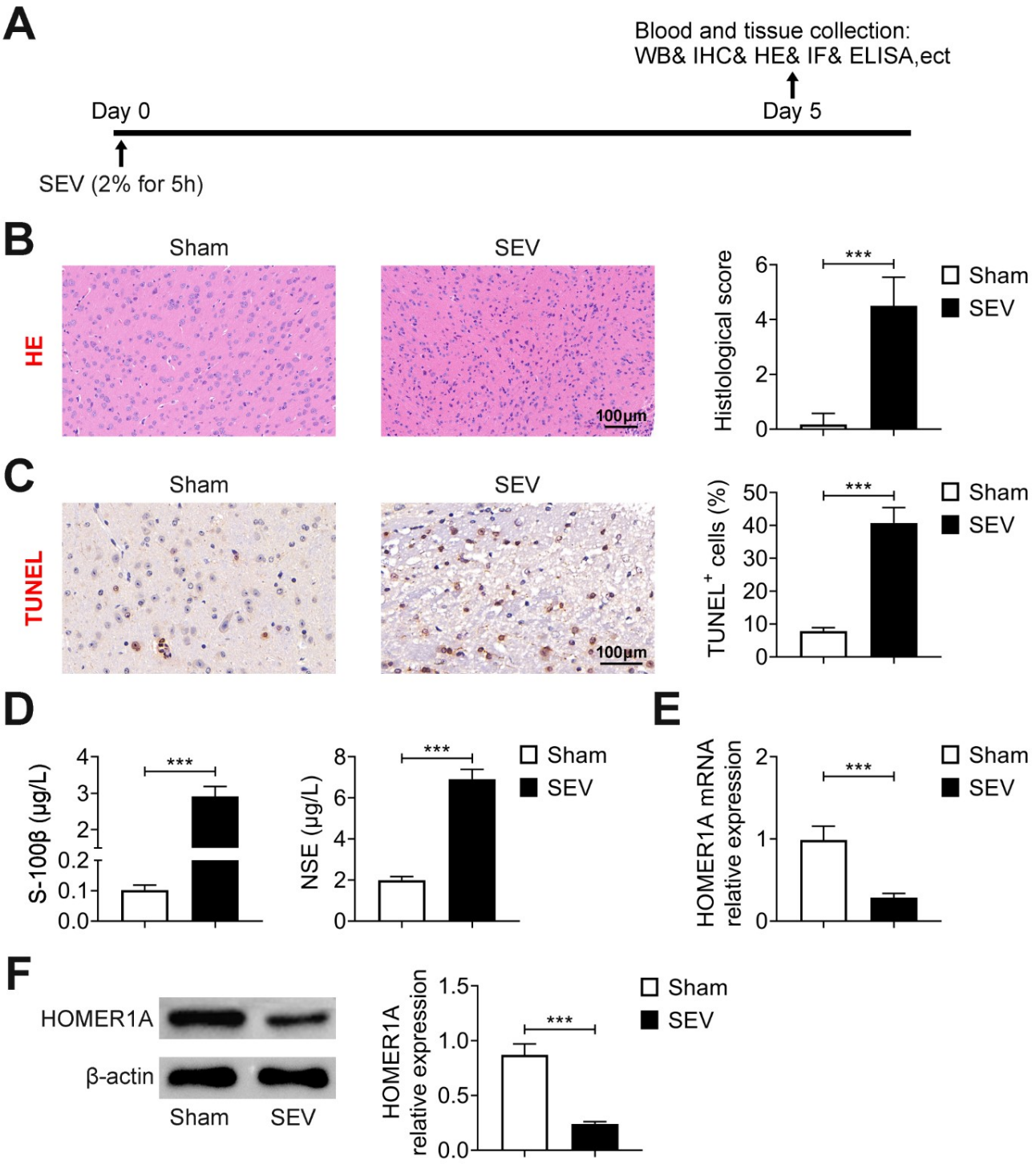

FIGURE 1. ***HOMER1A*** **exhibited lower expression in the brain tissues of SEV-induced rats.** (A) The schematic of the timeline was showed. SEV (2% for 5 h) was treated to rats at Day 0, and rats were killed at Day 5 to collect the blood and tissues for next experiments. (B) The damage of brain tissues in rats was detected in the Sham and SEV groups through H&E staining. (C) The cell apoptosis was measured in the Sham and SEV groups through TUNEL staining. (D) The levels of S-100β and NSE were assessed through ELISA. (E,F) The mRNA and protein expressions of HOMER1A were examined through RT-qPCR and western blot. Six rats were used in each group. ***$p < 0.001$. SEV: Sevoflurane; NSE: neuron-specific enolase.

treated with SEV (2% for 5 h) at Day 0, and the MVM test was done at day 2–5, and then rats were sacrificed at Day 5 to collect the blood and tissues for following experiments. Moreover, through IF assay, it was revealed that AAV-HOMER1A preferentially targeted astrocytes (GFAP) and microglia (IBA1) (**Supplementary Fig. 1**). The HOMER1A protein expression was up-regulated after overexpressing *HOMER1A* (Fig. 2B). Moreover, the damage of brain tissues was relieved after *HOMER1A* overexpression in SEV-treated rats, but not changed in the Sham rats (Fig. 2C). Additionally, the TUNEL positive cells were decreased after *HOMER1A* overexpression in SEV-treated rats, but not changed in the Sham rats (Fig. 2D). The levels of S-100β and NSE were reduced after *HOMER1A* overexpression in SEV-treated rats, but not changed in the Sham rats (Fig. 2E). The mRNA expressions of ApoE4 and Clec7a were both decreased after *HOMER1A* overexpression in SEV-treated rats, but not changed in the Sham rats (Fig. 2F). Similarly, we also discovered that the escape latency(s) was decreased, and the clutter level of path, time in target quadrant(s), number of platform crossings, distance covered in the target quadrant were all increased after overexpressing *HOMER1A* in SEV-treated rats, but not changed in the Sham rats (Fig. 2G). Taken together, *HOMER1A* ameliorated nerve injury and cognitive deficit in SEV-treated rats.

3.3 *HOMER1A* improved inflammation in the brain tissues of SEV-induced rats

Further experiments from RT-qPCR and ELISA demonstrated that the levels of TNF-α, IL-6 and IL-1β were enhanced after SEV treatment and their levels were decreased after overexpressing *HOMER1A* in SEV-induced rats, but not changed in the Sham rats (Fig. 3A,B). In addition, the NF-κB/p65 pathway (associated with inflammation) was assessed. Results uncovered that the expressions of p-NF-κB p65/NF-κB p65 were up-regulated after SEV treatment, and their levels were down-regulated after *HOMER1A* overexpression in SEV-induced rats, but not changed in the Sham rats (Fig. 3C). To sum up, *HOMER1A* improved inflammation in the brain tissues of SEV-induced rats.

3.4 *HOMER1A* reduced SEV-stimulated microglial activation

Next, through IF assay, it was demonstrated that the Iba1 level was obviously strengthened after SEV treatment and the Iba1 level was weakened after *HOMER1A* overexpression in SEV-induced rats, but not changed in the Sham rats (Fig. 4A). Furthermore, the M1 ($Iba1^+$ $CD16^+$) cells were increased after treated with SEV, and they were decreased after *HOMER1A* overexpression in SEV-induced rats, but not changed in the Sham rats. The M2 ($Iba1^+$ $Arg1^+$) cells were increased after treating with SEV and they were further increased after *HOMER1A* overexpression in SEV-induced rats, but not changed in the Sham rats (Fig. 4B). The Iba1, CD16, iNOS (M1-like marker), CD206 and Arg1 (M2-like marker) expressions were all enhanced after cells treated with SEV. The Iba1, CD16, iNOS (M1-like marker) expressions were reduced, but CD206 and Arg1 (M2-like marker) expressions were further increased after *HOMER1A* overexpression in SEV-induced rats, but not changed in the Sham rats (Fig. 4C). Additionally, the protein expressions of P2RY12 and TMEM119 were decreased after *HOMER1A* overexpression in SEV-induced rats, but not changed in the Sham rats (Fig. 4D). These findings disclosed that *HOMER1A* reduced SEV-stimulated microglial activation.

3.5 *HOMER1A* stimulated AMPK/TXNIP activation

As shown in Fig. 5A, the protein level of p-AMPK/AMPK was down-regulated after SEV treatment and its level was up-regulated after overexpressing *HOMER1A* in SEV-induced rats, but not changed in the Sham rats. The TXNIP protein expression was enhanced after SEV treatment, and its level was reduced after *HOMER1A* overexpression in SEV-induced rats, but not changed in the Sham rats. Additionally, the decreased expression of TXNIP mediated by *HOMER1A* overexpression in SEV-induced rats was reversed by CC (20 mg/kg, AMPK inhibitor) treatment (Fig. 5B). In short, *HOMER1A* activated AMPK pathway to reduce TXNIP expression.

3.6 Inhibition of AMPK activation attenuated the neuroprotective effects of *HOMER1A*

The reduced levels S-100β and NSE mediated by *HOMER1A* overexpression were rescued after treating with CC (Fig. 6A). Besides, *HOMER1A* overexpression down-regulated *TNF-α*, *IL-6* and *IL-1β* mRNA expressions, but this effect was restored by adding with CC (Fig. 6B). The decreased expressions of Iba1, CD16, iNOS, as well as the increased expression of CD206, Arg1 mediated by *HOMER1A* overexpression were reversed by CC treatment (Fig. 6C). Moreover, the decreased escape latency(s) was, and the increased clutter level of path, time in target quadrant(s), number of platform crossings, distance covered in the target quadrant mediated by *HOMER1A* overexpression were rescued after CC treatment (**Supplementary Fig. 2**). In addition, the decreased M1 ($Iba1^+$ $CD16^+$) cells, and the increased M2 ($Iba1^+$ $Arg1^+$) cells stimulated by *HOMER1A* overexpression were offset after CC addition (**Supplementary Fig. 3**). In general, inhibition of AMPK activation attenuated the neuroprotective effects of *HOMER1A*.

4. Discussion

Many anesthetics have been found to induce cognitive dysfunction. For example, suppression of microRNA-34a relieves propofol anesthesia-stimulated neurotoxicity and cognitive dysfunction through the MAPK/ERK pathway [19]. Moreover, Remimazolam regulates glutamate excitotoxicity to induce cognitive dysfunction in mice [20]. Additionally, Cucurbitacin E relieves SEV stimulated-cognitive dysfunction in rats through the NF-κB pathway [21]. Besides, in neonatal mice with cognitive dysfunction triggered by SEV, deletion of *TLR3* reduces programmed necrosis of brain cells [22]. SEV is a common inhaled anesthetics utilized in surgery [4], which could result in cognitive dysfunction. Therefore, SEV was

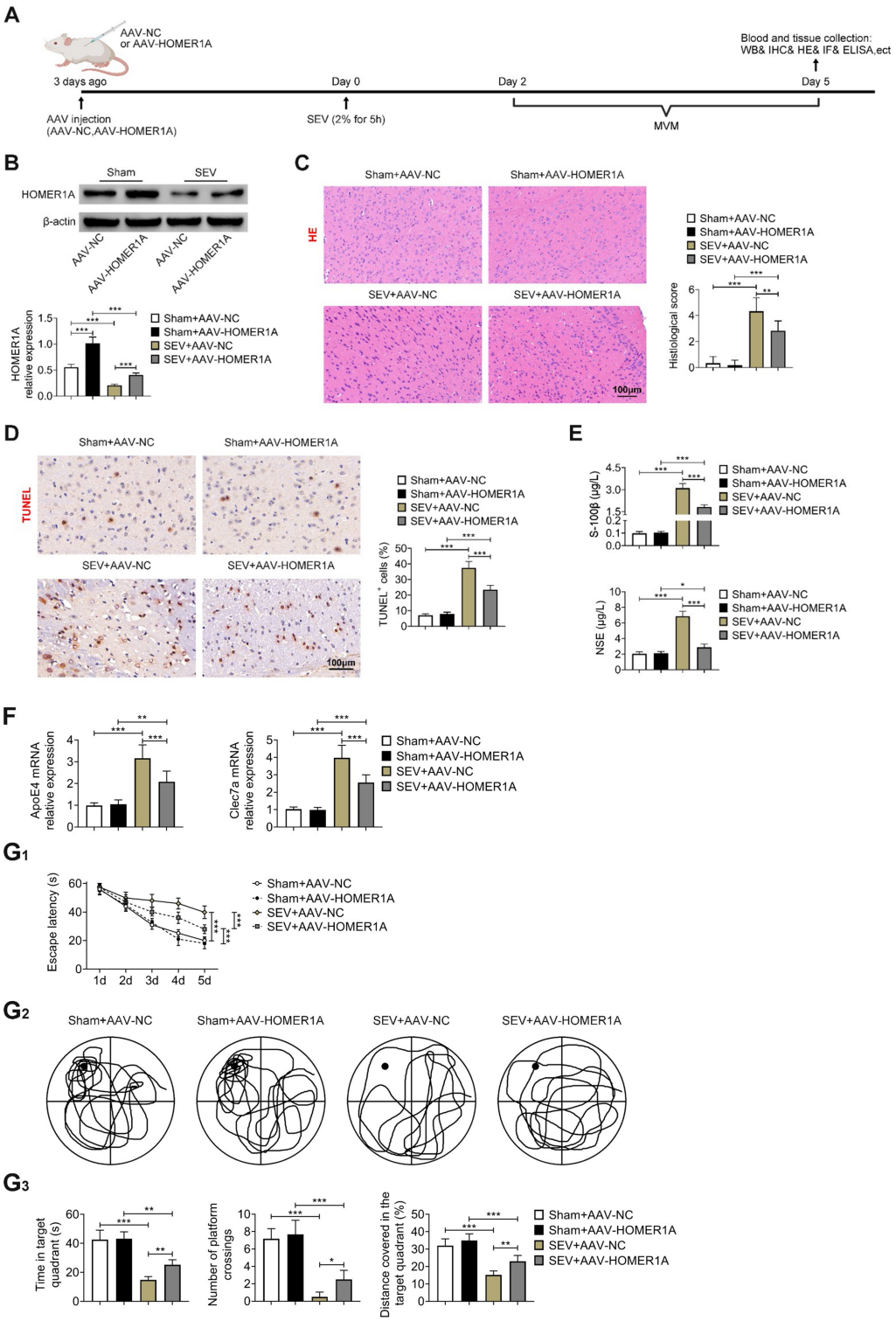

FIGURE 2. ***HOMER1A*** **ameliorated nerve injury and cognitive deficit in SEV-induced rats.** (A) The schematic of the timeline was showed. 3 days ago, AAV-NC or AAV-HOMER1A was injected into the rats. SEV (2% for 5 h) was treated to rats at Day 0, the MVM test was done at Day 2–5, and rats were killed at Day 5 to collect the blood and tissues for next experiments. Groups were divided into the Sham + AAV-NC, Sham + AAV-HOMER1A, SEV + AAV-NC and SEV + AAV-HOMER1A group. (B) The protein expression of HOMER1A was measured through western blot. (C) The damage of brain tissues was evaluated through H&E staining. (D) The cell apoptosis was examined through TUNEL assay. (E) The S-100β and NSE levels were tested through ELISA. (F) The mRNA expressions of *ApoE4* and *Clec7a* were detected through RT-qPCR. (G_{1-3}) The Escape latency, Clutter level of path, Time in target quadrant, Number of platform crossings, Distance covered in the target quadrant were assessed through Morris water maze test. Six rats were used in each group. $^{*}p < 0.05$, $^{**}p < 0.01$ and $^{***}p < 0.001$. SEV: Sevoflurane; AAV: adeno-associated virus.

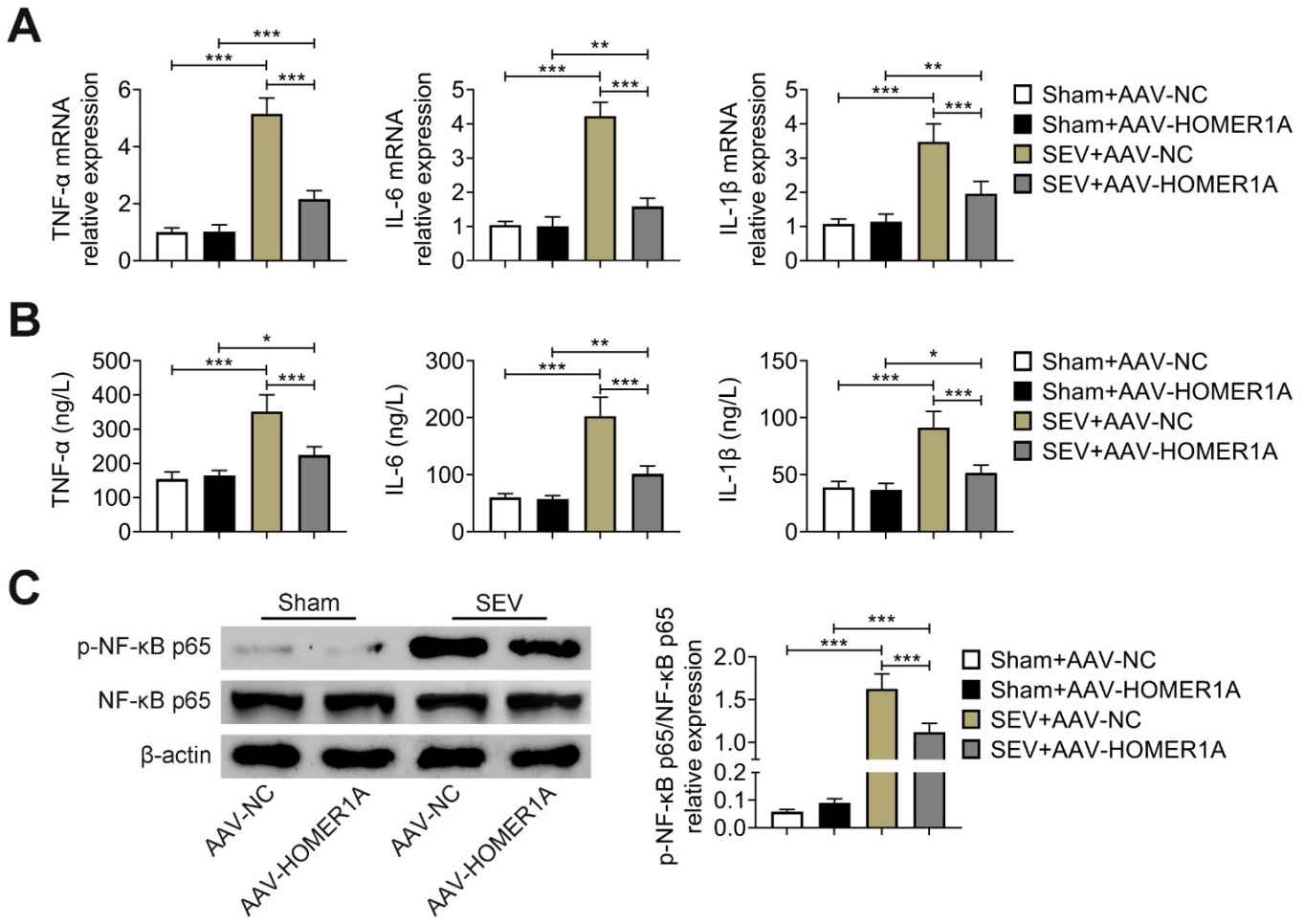

FIGURE 3. *HOMER1A* improved inflammation in the brain tissues of SEV-induced rats. (A) The TNF-α, IL-6 and IL-1β mRNA expressions were measured through RT-qPCR. (B) The TNF-α, IL-6 and IL-1β levels were detected through ELISA. (C) The expression of p-NF-κB p65/NF-κB p65 was tested through western blot. Six rats were used in each group. *$p < 0.05$, **$p < 0.01$ and ***$p < 0.001$. SEV: Sevoflurane; AAV: adeno-associated virus; TNF-α: tumor necrosis factor-α; IL-6: Interleukin-6; IL-1β: Interleukin-1β.

used in our study. First, the rat model was established through inhaling 2% SEV. Similar to these above studies, results from our study uncovered that the brain tissues of SEV-treated rats were severely damaged, and the levels of S-100β and NSE were markedly elevated after SEV treatment.

HOMER1A has been uncovered to own neuroprotective effect to reduce neuronal injury [12, 23]. However, the regulatory role of *HOMER1A* in anesthetic-stimulated cognitive impairment needs more explorations. In this work, it was confirmed that *HOMER1A* exhibited lower expression in the brain tissues of SEV-treated rats. In addition, *HOMER1A* ameliorated nerve injury and cognitive deficit in SEV-treated rats.

Microglia are myeloid cells existed in the central nervous system (CNS) and are essential for healthy brain function [24]. Microglia are neuronal protectors of the microenvironment and can be easily activated through immune stimulation, toxin, or injury [25]. Microglia function is similar to macrophages in the brain, and under the normal physiological condition, there are M1 microglia (pro-inflammatory) and M2 microglia (anti-inflammatory) [26]. Therefore, the study of microglia is the core of neuroinflammation research. One study has revealed that anesthetic isoflurane stimulates the activation of microglia in the hippocampal region of animals and converts it to the M1 phenotype, which results in inflammatory responses and nerve damage [27]. In this study, *HOMER1A* improved inflammation through reducing the levels of inflammatory factors and blocking the NF-κB p65 pathway in the brain tissues of SEV-induced rats. Furthermore, *HOMER1A* suppressed SEV-stimulated microglial activation through modulating M1/M2 polarization.

AMP-activated protein kinase (AMPK) affects cell growth, the balance energy metabolism and other processes [11]. On the one side, AMPK activation can alleviate cognitive impairment mediated by neuronal apoptosis. In addition, AMPK activation can suppress TXNIP expression, retard microglia activation and mitigate neuroinflammatory response [28]. AMPK has been disclosed to take part in SEV-mediated cognitive dysfunction. For instance, *CTRP3* affects the AMPK/SIRT1 and PI3K/AKT pathways to attenuate SEV anesthesia-triggered cognitive dysfunction [29]. AMPK-SIRT1 pathway facilitates SEV-stimulated neuron apoptosis and cognitive impair-

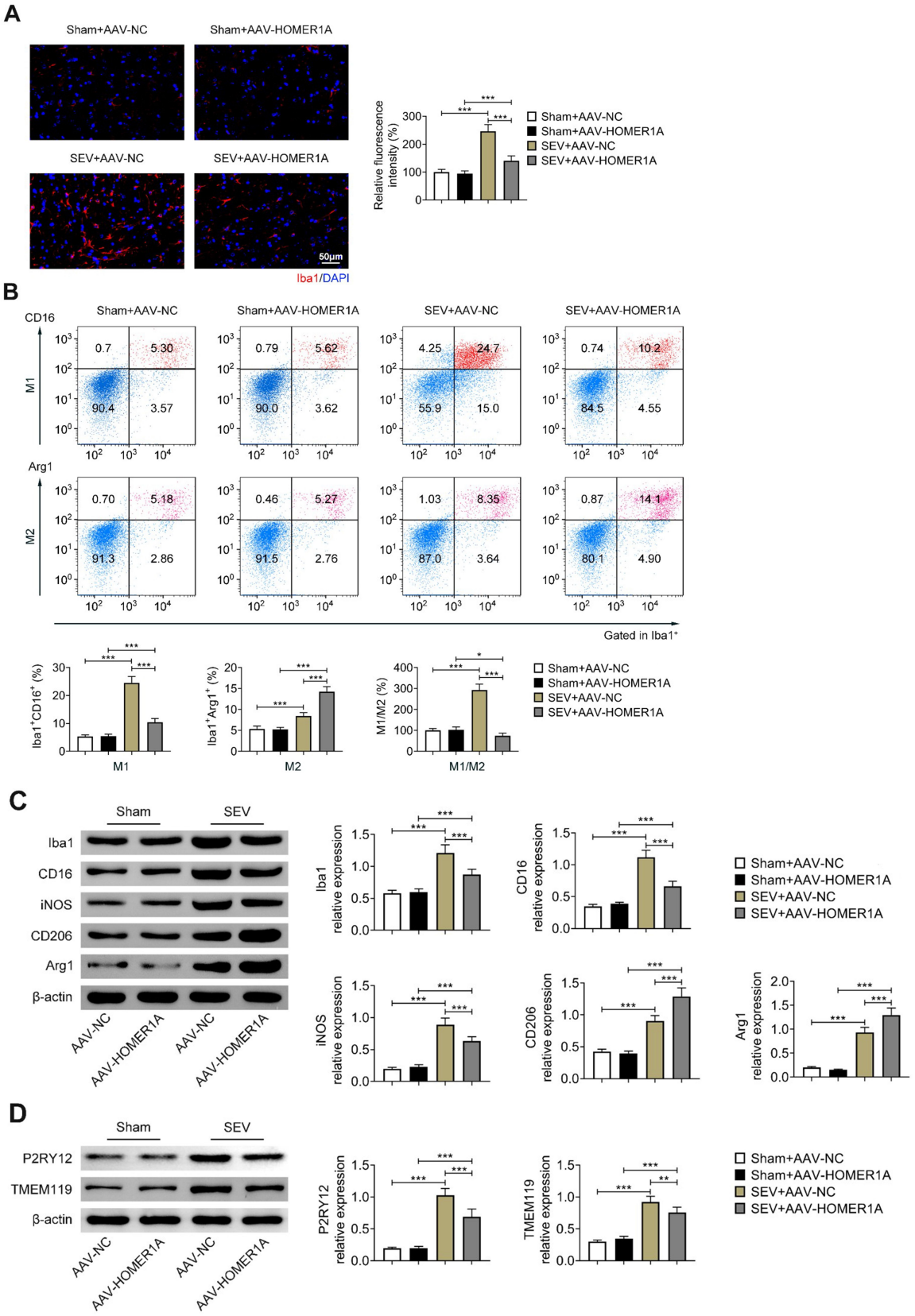

FIGURE 4. ***HOMER1A*** **reduced SEV-induced microglial activation.** Groups were divided into the Sham + AAV-NC, Sham + AAV-HOMER1A, SEV + AAV-NC and SEV + AAV-HOMER1A group. (A) The Iba1 level was evaluated through IF assay. (B) The M1 ($Iba1^+$ $CD16^+$) and M2 ($Iba1^+$ $Arg1^+$) cells were confirmed through flow cytometry. (C) The Iba1, CD16, iNOS (M1-like marker), CD206 and Arg1 (M2-like marker) expressions were assessed through western blot. (D) The protein expressions of P2RY12 and TMEM119 were evaluated through western blot. Six rats were used in each group. $^{**}p < 0.01$, $^{***}p < 0.001$. SEV: Sevoflurane; AAV: adeno-associated virus.

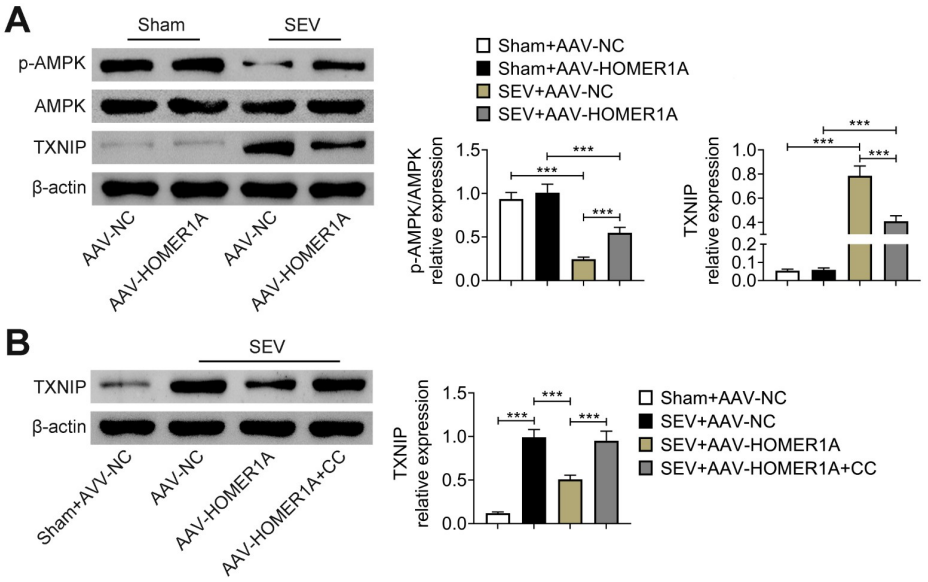

FIGURE 5. ***HOMER1A* stimulated AMPK/TXNIP activation.** (A) The p-AMPK/AMPK and TXNIP levels were examined in the Sham + AAV-NC, Sham + AAV-HOMER1A, SEV + AAV-NC and SEV + AAV-HOMER1A groups through western blot. (B) The TXNIP expression was tested in the Sham, SEV + AAV-NC, SEV + AAV-HOMER1A and SEV + AAV-HOMER1A + CC (AMPK inhibitor) groups through western blot. Six rats were used in each group. ***$p < 0.001$. SEV: Sevoflurane; AAV: adeno-associated virus.

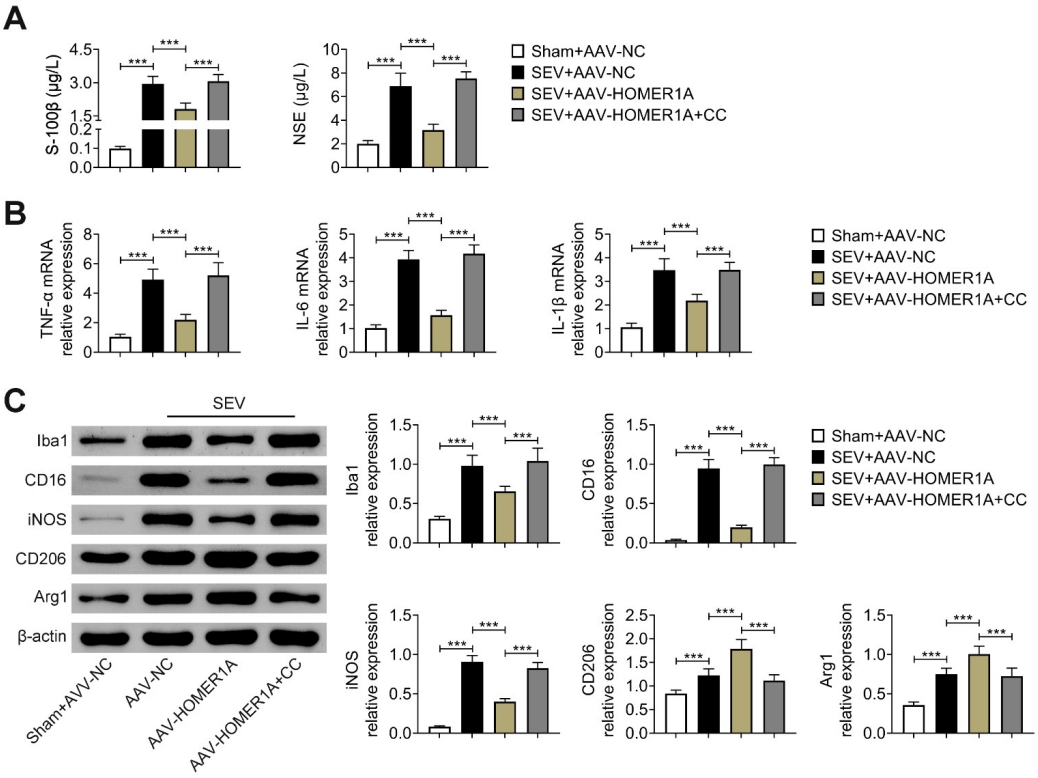

FIGURE 6. Inhibition of AMPK activation attenuated the neuroprotective effects of *HOMER1A*. Groups were divided into the Sham, SEV + AAV-NC, SEV + AAV-HOMER1A and SEV + AAV-HOMER1A + CC (AMPK inhibitor) group. (A) The S-100β and NSE levels were assessed through ELISA. (B) The *TNF-*α, *IL-6* and *IL-1*β mRNA expressions were examined through RT-qPCR. (C) The Iba1, CD16, iNOS (M1-like marker), CD206 and Arg1 (M2-like marker) expressions were tested through western blot. Six rats were used in each group. ***$p < 0.001$. SEV: Sevoflurane; AAV: adeno-associated virus; TNF-α: tumor necrosis factor-α; IL-6: Interleukin-6; IL-1β: Interleukin-1β.

ment [30]. AMPKα1 affects AMPK-Sirt1 and autophagy signaling to ameliorate postoperative cognitive dysfunction [31]. Importantly, it was identified that *HOMER1A* activates AMPK-dependent autophagy to reduce hydrogen peroxide-stimulated oxidative damage [32]. In this study, our results demonstrated that *HOMER1A* activated AMPK pathway to reduce TXNIP expression. Finally, through rescue assays, inhibition of AMPK activation (CC treatment) attenuated the neuroprotective effects of *HOMER1A* in SEV-triggered rats.

5. Conclusions

It was the first time to uncover that *HOMER1A* regulated microglia M1/M2 polarization to restore SEV-stimulated cognitive dysfunction through activating the AMPK/TXNIP axis. Nevertheless, some limitations have existed into this work, such as missing clinical samples and other cellular progresses. In the future, more explorations associated with *HOMER1A* in SEV-stimulated cognitive dysfunction will be conducted to elucidate its other roles.

AVAILABILITY OF DATA AND MATERIALS

All data generated or analyzed during this study are included in this published article.

AUTHOR CONTRIBUTIONS

GZZ—designed the research study, performed the research. JMJ—analyzed the data, wrote the manuscript. All authors read and approved the final manuscript.

ETHICS APPROVAL AND CONSENT TO PARTICIPATE

Ethical approval was obtained from the Ethics Committee of Shanxi Provincial People's Hospital (Approval No. 2022-88).

ACKNOWLEDGMENT

Not applicable.

FUNDING

This research received no external funding.

CONFLICT OF INTEREST

The authors declare no conflict of interest.

SUPPLEMENTARY MATERIAL

Supplementary material associated with this article can be found, in the online version, at https://oss.signavitae.com/mre-signavitae/article/1677208691577634816/attachment/Supplementary%20material.docx.

REFERENCES

[1] Wang CM, Chen WC, Zhang Y, Lin S, He HF. Update on the mechanism and treatment of sevoflurane-induced postoperative cognitive dysfunction. Frontiers in Aging Neuroscience. 2021; 13: 702231.

[2] Liu J, Huang K, Zhu B, Zhou B, Ahmad Harb AK, Liu L, *et al*. Neuropsychological tests in post-operative cognitive dysfunction: methods and applications. Frontiers in Psychology. 2021; 12: 684307.

[3] Yu H, Kang H, Fan J, Cao G, Liu B. Influence of dexmedetomidine on postoperative cognitive dysfunction in the elderly: a meta-analysis of randomized controlled trials. Brain and Behavior. 2022; 12: e2665.

[4] Palanca BJA, Avidan MS, Mashour GA. Human neural correlates of sevoflurane-induced unconsciousness. British Journal of Anaesthesia. 2017; 119: 573–582.

[5] Sun M, Xie Z, Zhang J, Leng Y. Mechanistic insight into sevoflurane-associated developmental neurotoxicity. Cell Biology and Toxicology. 2022; 38: 927–943.

[6] Yang X, Zhang W, Wu H, Fu S, Yang J, Liu S, *et al*. Downregulation of CDK5 restores sevoflurane-induced cognitive dysfunction by promoting SIRT1-mediated autophagy. Cellular and Molecular Neurobiology. 2020; 40: 955–965.

[7] Wei W, Sun Z, He S, Zhang W, Chen S. Protective role of dexmedetomidine against sevoflurane-induced postoperative cognitive dysfunction *via* the microRNA-129/TLR4 axis. Journal of Clinical Neuroscience. 2021; 92: 89–97.

[8] Yu Y, Zhang W, Zhu D, Wang H, Shao H, Zhang Y. LncRNA Rian ameliorates sevoflurane anesthesia-induced cognitive dysfunction through regulation of miR-143-3p/LIMK1 axis. Human Cell. 2021; 34: 808–818.

[9] He B, Wang J. METTL3 regulates hippocampal gene transcription *via* N6-methyladenosine methylation in sevoflurane-induced postoperative cognitive dysfunction mouse. Aging. 2021; 13: 23108–23118.

[10] Ahmad Hariza AM, Mohd Yunus MH, Murthy JK, Wahab S. Clinical improvement in depression and cognitive deficit following electroconvulsive therapy. Diagnostics. 2023; 13: 1585.

[11] Reshetnikov VV, Bondar NP. The role of stress-induced changes of Homer1 expression in stress susceptibility. Biochemistry. 2021; 86: 613–626.

[12] Wang Y, Zhao M, Shang L, Zhang Y, Huang C, He Z, *et al*. Homer1a protects against neuronal injury *via* PI3K/AKT/mTOR signaling pathway. International Journal of Neuroscience. 2020; 130: 621–630.

[13] Fei F, Li J, Rao W, Liu W, Chen X, Su N, *et al*. Upregulation of Homer1a promoted retinal ganglion cell survival after retinal ischemia and reperfusion *via* interacting with Erk pathway. Cellular and Molecular Neurobiology. 2015; 35: 1039–1048.

[14] Serchov T, Schwarz I, Theiss A, Sun L, Holz A, Döbrössy MD, *et al*. Enhanced adenosine A_1 receptor and Homer1a expression in hippocampus modulates the resilience to stress-induced depression-like behavior. Neuropharmacology. 2020; 162: 107834.

[15] Tappe A, Klugmann M, Luo C, Hirlinger D, Agarwal N, Benrath J, *et al*. Synaptic scaffolding protein Homer1a protects against chronic inflammatory pain. Nature Medicine. 2006; 12: 677–681.

[16] Orihuela R, McPherson CA, Harry GJ. Microglial M1/M2 polarization and metabolic states. British Journal of Pharmacology. 2016; 173: 649–665.

[17] Iadecola C, Anrather J. The immunology of stroke: from mechanisms to translation. Nature Medicine. 2011; 17: 796–808.

[18] Shan W, Nagai T, Tanaka M, Itoh N, Furukawa-Hibi Y, Nabeshima T, *et al*. Neuronal PAS domain protein 4 (Npas4) controls neuronal homeostasis in pentylenetetrazole-induced epilepsy through the induction of Homer1a. Journal of Neurochemistry. 2018; 145: 19–33.

[19] Li GF, Li ZB, Zhuang SJ, Li GC. Inhibition of microRNA-34a protects against propofol anesthesia-induced neurotoxicity and cognitive dysfunction *via* the MAPK/ERK signaling pathway. Neuroscience Letters. 2018; 675: 152–159.

[20] Zhou X, Zhang C, Wang L, Jin S. Remimazolam induced cognitive dysfunction in mice *via* glutamate excitotoxicity. Translational Neuroscience. 2022; 13: 104–115.

[21] Zheng S, Shi B, Li X, Yuan H, Feng Y. Cucurbitacin E reduces the

cognitive dysfunction induced by sevoflurane in rats by regulating NF-κB pathway. Acta Biochimica Polonica. 2022; 69: 387–391.

[22] Zhang Q, Li Y, Yu J, Yin C, Guo J, Zhao J, *et al*. TLR3 deletion inhibits programmed necrosis of brain cells in neonatal mice with sevoflurane-induced cognitive dysfunction. Aging. 2022; 14: 4714–4727.

[23] Fei Z, Fei F, Wu X, Su N. Homer signaling pathways as effective therapeutic targets for ischemic and traumatic brain injuries and retinal lesions. Neural Regeneration Research. 2022; 17: 1454.

[24] Guo S, Wang H, Yin Y. Microglia polarization from M1 to M2 in neurodegenerative diseases. Frontiers in Aging Neuroscience. 2022; 14: 815347.

[25] Lukens JR, Eyo UB. Microglia and neurodevelopmental disorders. Annual Review of Neuroscience. 2022; 45: 425–445.

[26] Xu L, He D, Bai Y. Microglia-mediated inflammation and neurodegenerative disease. Molecular Neurobiology. 2016; 53: 6709–6715.

[27] Jiang T, Xu S, Shen Y, Xu Y, Li Y. Genistein attenuates isoflurane-induced neuroinflammation by Inhibiting TLR4-mediated microglial-polarization *in vivo* and *in vitro*. Journal of Inflammation Research. 2021; 14: 2587–2600.

[28] Yu J, Wang W, Matei N, Li X, Pang J, Mo J, *et al*. Ezetimibe attenuates oxidative stress and neuroinflammation *via* the AMPK/Nrf2/TXNIP pathway after MCAO in rats. Oxidative Medicine and Cellular Longevity. 2020; 2020: 1–14.

[29] Yang LH, Xu YC, Zhang W. Neuroprotective effect of CTRP3 overexpression against sevoflurane anesthesia-induced cognitive dysfunction in aged rats through activating AMPK/SIRT1 and PI3K/AKT signaling pathways. European Review for Medical and Pharmacological Sciences. 2020; 24: 5091–5100.

[30] Liu L, Liu C, Fang L. AMPK-SIRT1 pathway dysfunction contributes to neuron apoptosis and cognitive impairment induced by sevoflurane. Molecular Medicine Reports. 2021; 23: 56.

[31] Yan W, Wang D, Ren D, Wang L, Hu Z, Ma Y, *et al*. AMPKα1 overexpression improves postoperative cognitive dysfunction in aged rats through AMPK-Sirt1 and autophagy signaling. Journal of Cellular Biochemistry. 2019; 120: 11633–11641.

[32] Wu X, Luo P, Rao W, Dai S, Zhang L, Ma W, *et al*. Homer1a attenuates hydrogen peroxide-induced oxidative damage in HT-22 cells through AMPK-dependent autophagy. Frontiers in Neuroscience. 2018; 12: 51.

How to cite this article: Guangzhen Zhao, Jianmin Jing. *HOMER1A* restores sevoflurane-induced cognitive dysfunction by regulating Microglia's activation through activating the AMPK/TXNIP axis. Signa Vitae. 2023; 19(4): 202-212. doi: 10.22514/sv.2023.065.